Expanded View Figures

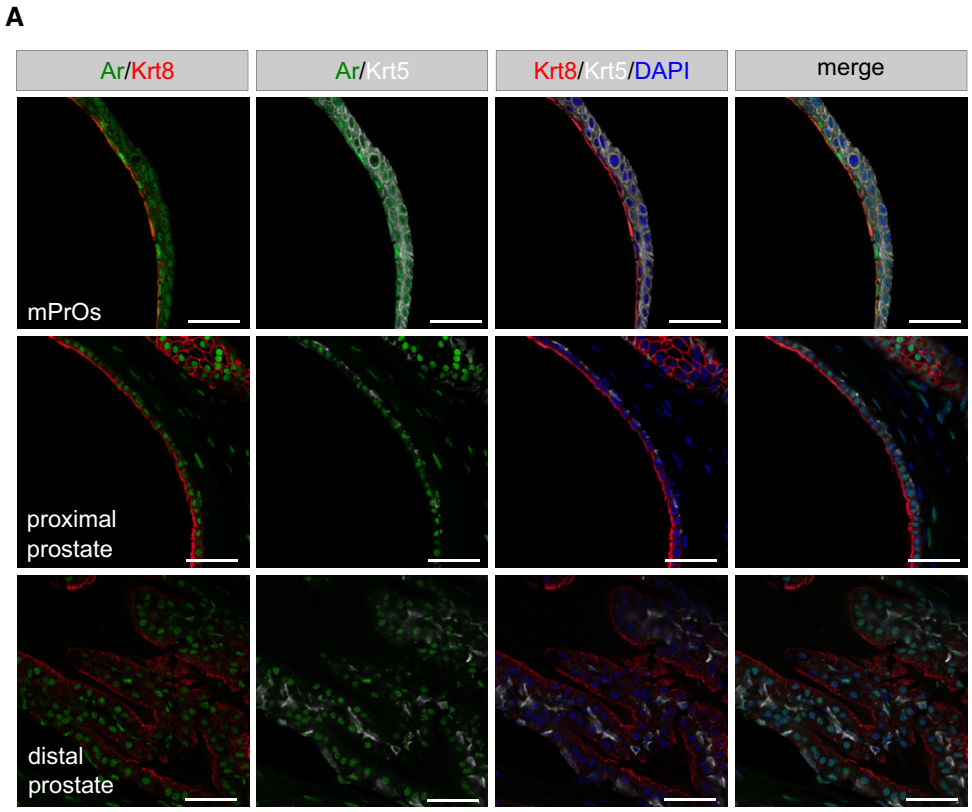

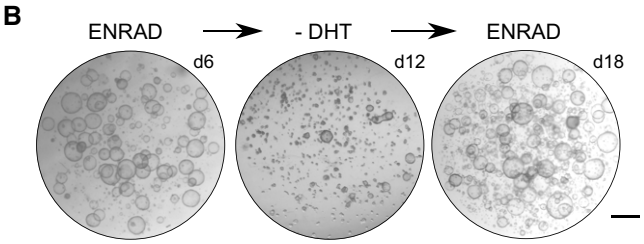

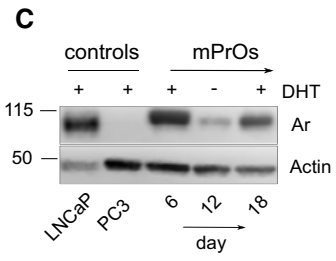

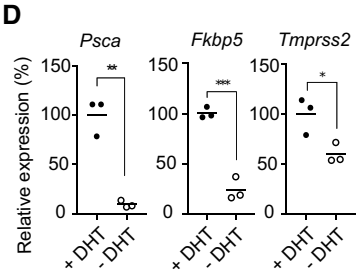

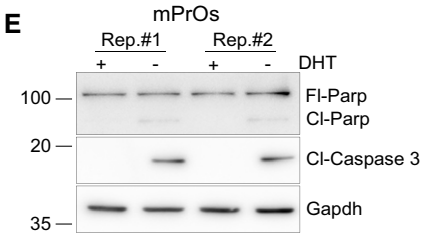

Figure EV1.

Figure EV1. Mouse prostate organoids are dependent on androgen signaling for lumen formation—but not for survival, related to Fig 1.

A Immunofluorescence analysis for selected markers in mouse prostate tissue and organoid sections. Scale bars = 50 μm.
B Stereoscopic images of mouse prostate organoids experiencing transient DHT removal (androgen cycling). Lumen formation necessitates androgen signaling. Scale bar = 1 mm.
C Western blot analysis for androgen receptor (Ar) expression in mouse prostate organoids experiencing androgen cycling, and control cell lines expressing (LNCaP) or not expressing (PC3) the receptor.
D qRT–PCR mRNA expression analysis for selected androgen-responsive genes in the presence or absence of DHT. Data points are shown with crossing line representing mean value (n = 3 biological replicates; Student's t-test, two-tailed, P-value *< 0.05, **< 0.01, ***< 0.001).
E Western blot analysis for apoptotic markers (Cleaved Caspase 3, Full-length, and Cleaved Parp) expression in mouse prostate organoids cultured with or without DHT (n = 2 biological replicates).

Source data are available online for this figure.

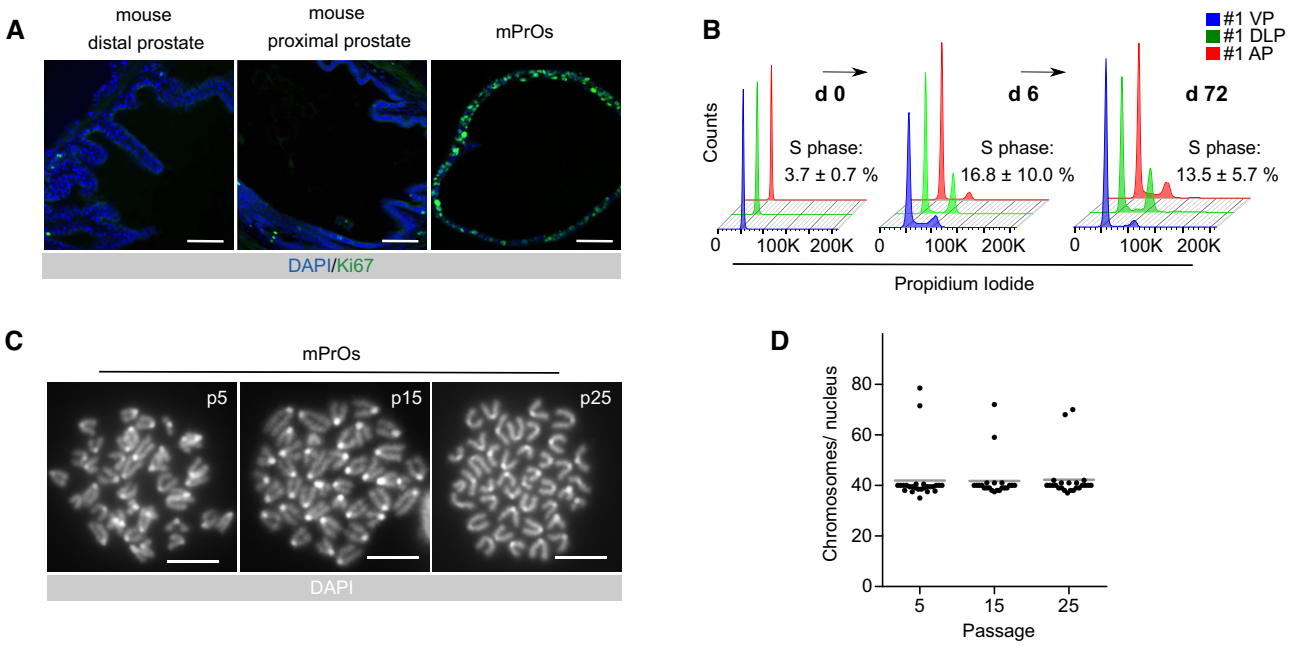

Figure EV2. Low levels of genomic instability in fast cycling mouse prostate organoids, related to Fig 1.

A Immunofluorescence staining for Ki67 in mouse prostate tissue and organoid sections. Scale bars = 50 μm.
B Flow cytometry analysis for DNA content.
C Representative karyotypes. Scale bars = 10 μm.
D Quantification of karyotype analysis. Data points are shown with crossing line representing mean value (n = 25 metaphases/passage).

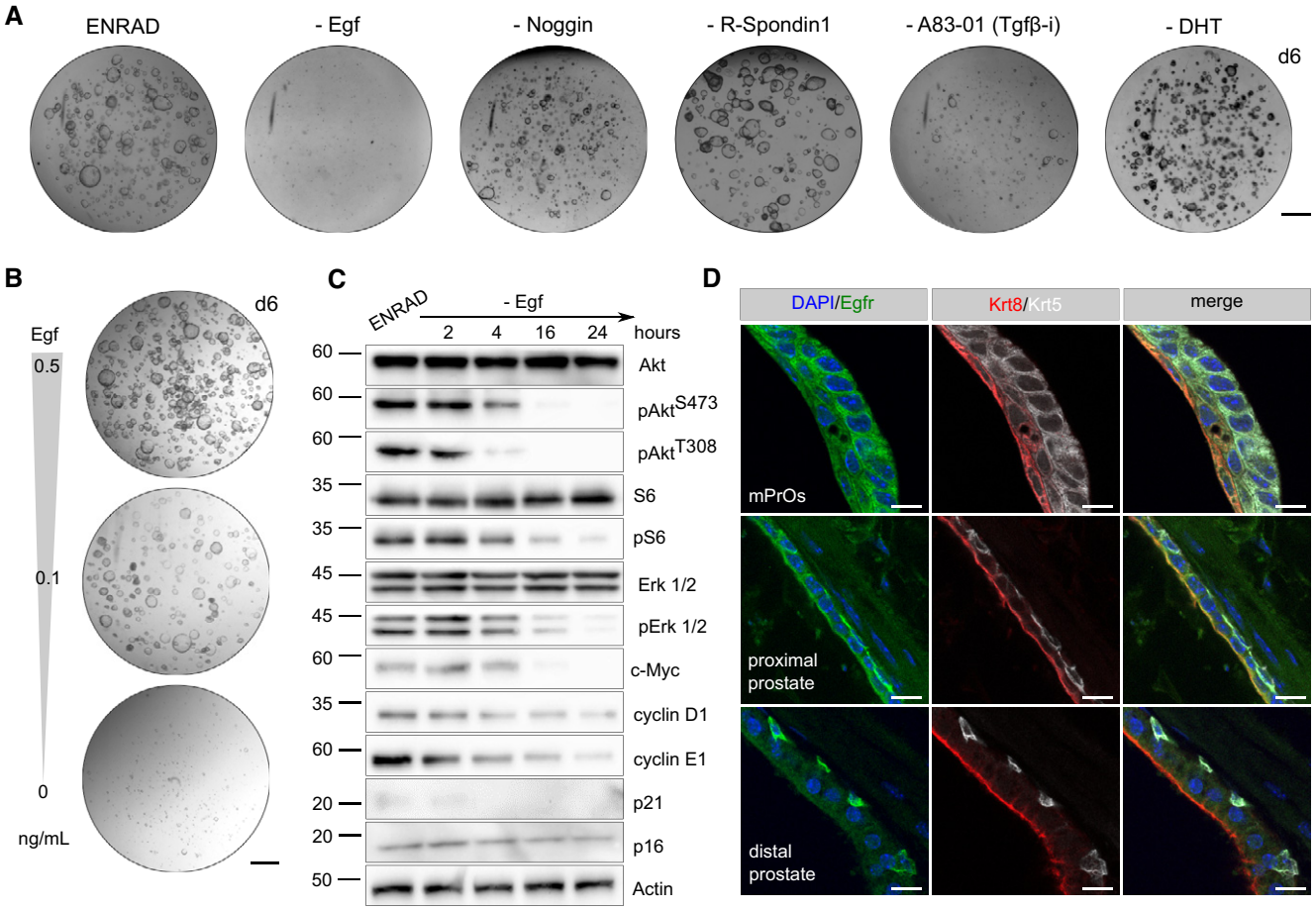

Figure EV3. Mouse prostate organoids rely on Egf signaling for continuous proliferation, related to Fig 1.

A Representative stereoscopic images of mouse prostate organoid grown in complete medium (ENRAD) vs. medium depleted of individual growth factors/inhibitors. Mouse prostate organoids necessitate of both Egf and the Tgf-β inhibitor A83-01 for continuous expansion. Within the period of observation, removal of Noggin or R-Spondin 1 has no clear consequence in culture. Please note that organoids failed to form a lumen in the absence of DHT. Scale bar = 1 mm.

B Stereoscopic images of mouse prostate organoids cultured in the presence of reduced levels (0.5, 0.1 ng/ml) or in the absence of Egf. Scale bar = 1 mm.

C Western blot analysis in mouse prostate organoids for selected signaling mediator and cell cycle regulator proteins.

D Immunofluorescence analysis for selected markers in mouse prostate tissue and organoid sections. Scale bars = 10 μm.

Source data are available online for this figure.

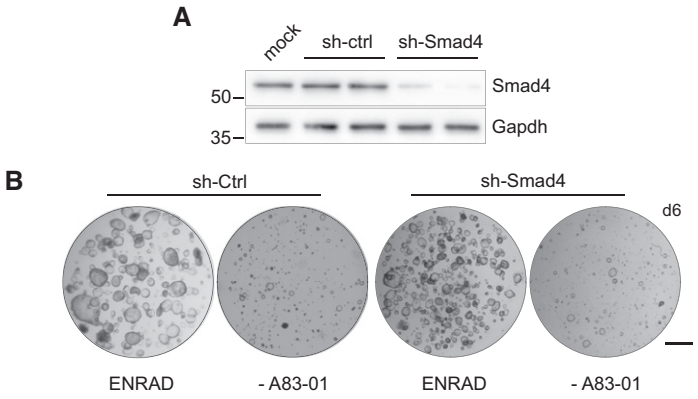

Figure EV4. Canonical Smad signaling is dispensable for Tgf-β induced quiescence in prostate organoids, related to Fig 2.

A Western blot analysis for Smad4 in mouse prostate organoids upon short-hairpin RNA mediated knockdown (sh-Smad4) and in control conditions (sh-Ctrl).

B Representative stereoscopic images of control (sh-Ctrl) and Smad4 knocked down (sh-Smad4) mouse prostate organoids in normal growth condition (ENRAD) and following A83-01 withdrawal (-A83-01). Scale bar = 1 mm.

Source data are available online for this figure.

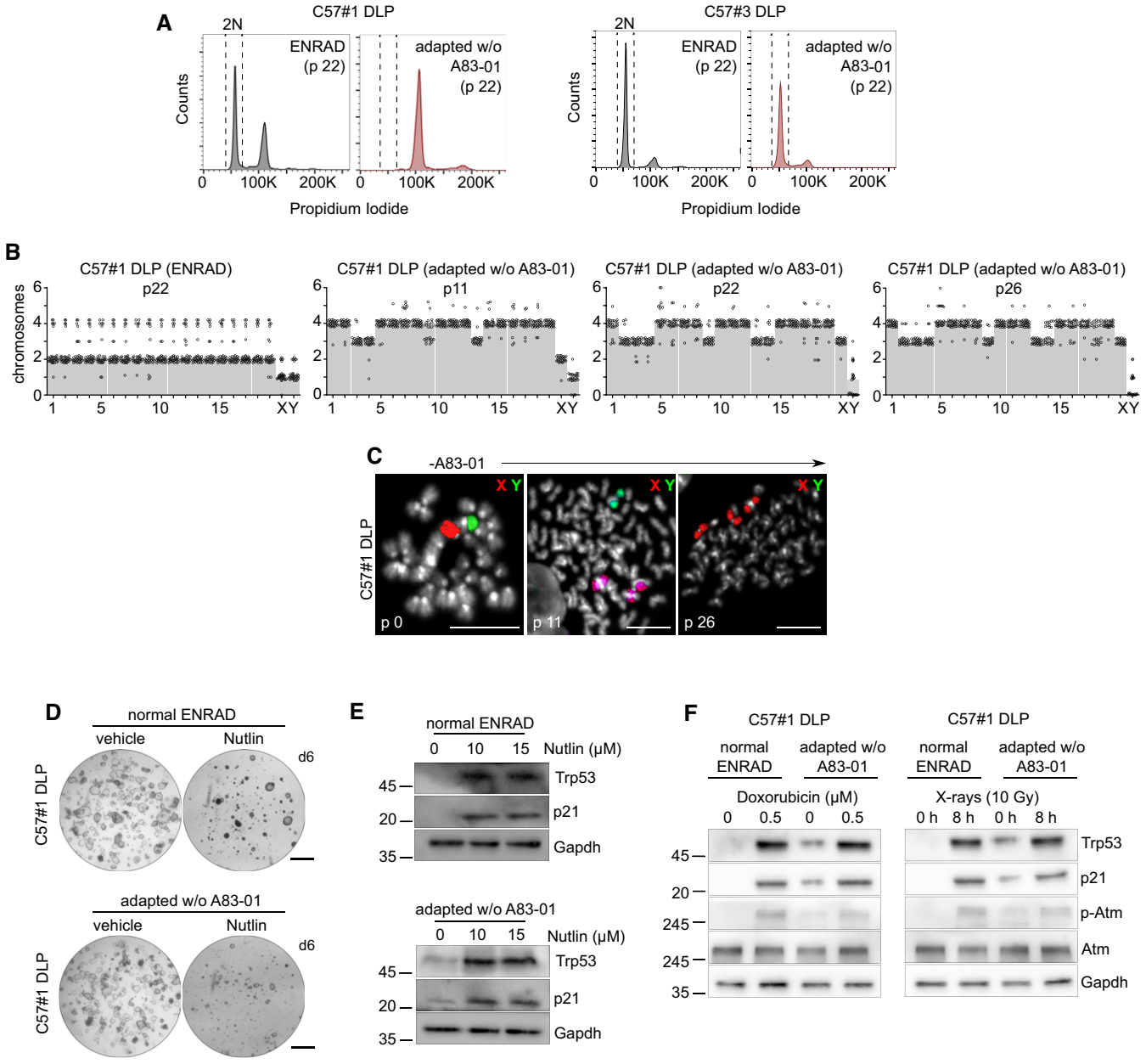

Figure EV5. C57#1 DLP mouse prostate organoids adapted to the absence of A83-01 in culture display widespread genomic instability while retaining intact p53 pathway, related to Fig 3.

A DNA content analysis in C57#1 DLP and C57#3 DLP mouse prostate organoid lines.

B Quantification of spectral karyotype (SKY) longitudinal analysis in C57#1 DLP mouse prostate organoids undergoing adaptation to the absence of A83-01 in culture (related to Fig 3F). During adaptation, an early genome duplication event is observed followed by selective chromosome loss and gains, and leading to subtetraploidy (n = 2 biological replicates, 25 metaphases/condition).

C Representative dual-color FISH images for X and Y chromosomes in C57#1 DLP mouse prostate organoids during adaptation to the absence of A83-01 in culture. This analysis confirmed a progressive sex chromosome imbalance during adaptation. Scale bars = 5 μm.

D Representative stereoscopic images of C57#1 DLP mouse prostate organoids treated with Nutlin, or vehicle as control. Scale bar = 1 mm.

E Western blot analysis of C57#1 DLP mouse prostate organoids described in (D).

F Western blot analysis in C57#1 DLP mouse prostate organoids treated with doxorubicin or X-rays. C57#1 DLP mouse prostate organoids retain a functional p53 pathway.

Source data are available online for this figure.